Tutorial

Koji Sugioka* and Ya Cheng*

A tutorial on optics for ultrafast laser materials processing: basic microprocessing system to beam shaping and advanced focusing methods

Abstract: Ultrafast lasers have excellent characteristics for materials processing in terms of precision and quality. This tutorial paper introduces the basic concepts of ultrafast laser materials processing and the structure and key components of typical ultrafast laser microprocessing systems. The emphasis is on the pulse-shaping devices and systems for controlling and manipulating the spatial, temporal, and polarization properties of focused femtosecond laser pulses.

Keywords: focusing optics; materials processing; spatial pulse shaping; temporal pulse shaping; ultrafast laser.

***Corresponding authors: Koji Sugioka,** Laser Technology Laboratory, RIKEN, Advanced Science Institute, 2-1 Hirosawa, Wako, Saitama 351-0198, Japan, e-mail: ksugioka@riken.jp; and
Ya Cheng, State Key Laboratory of High Field Laser Physics, Shanghai Institute of Optics and Fine Mechanics, Chinese Academy of Sciences, Shanghai 201800, China, e-mail: ya.cheng@siom.ac.cn

1 Introduction

The term ultrafast lasers is generally used to refer to lasers that emit pulses with durations in the range of femtoseconds (10^{-15} s) to a few tens of picoseconds (10^{-12} s). Ultrafast lasers were first employed for materials processing in the late 1980s when Srinivasan et al. [1] and Küper and Stuke [2] used femtosecond ultraviolet excimer lasers to ablate polymethylmethacrylate (PMMA). They demonstrated clean ablation with little formation of heat-affected zones (HAZs). In the mid-1990s, Hirao's group [3] and Mazur's group [4] pioneered the internal modification of transparent materials using tightly focused femtosecond near-infrared laser pulses. They demonstrated the refractive index modification in various glass materials. Owing to these unique capabilities, the ultrafast lasers are commonly used for materials processing both in fundamental investigations and various applications.

An important feature of ultrafast laser materials processing is that it can achieve extremely high precision (e.g., feature sizes down to ~20 nm) due to the efficient suppression of the heat diffusion to the surrounding regions of the processed area [5, 6]. From an optical point of view, such high precision imposes very stringent requirements on the spatial and temporal characteristics of the laser pulses. On the other hand, as the temporal profiles of ultrafast laser pulses can be tailored with temporal resolutions (e.g., the smallest temporal features of tailored pulses) far exceeding the characteristic energy transfer times, temporal pulse shaping has become an efficient way to precisely control the dynamics of energy deposition in materials, significantly improving the fabrication quality [7]. These challenges and opportunities provide strong incentives to develop optical devices and systems for ultrafast laser materials processing with the main aims of improving the resolution, throughput, and surface quality.

Although both picosecond and femtosecond lasers are now widely used for the ultrafast laser processing, the spatiotemporal properties of the femtosecond laser pulses can be controlled to a higher degree, and the femtosecond lasers can be used to perform three-dimensional (3D) fabrication within transparent materials. This paper particularly emphasizes the optics for the femtosecond laser processing. The remainder of this paper is organized as follows. Section 2 introduces the characteristics of ultrafast laser processing. Section 3 describes the typical systems for femtosecond laser materials processing. Section 4 reviews the various pulse-shaping techniques, including temporal pulse shaping, spatial pulse shaping, spatiotemporal pulse shaping, and pulse polarization shaping. Finally, the summary and future outlook are given in Section 5.

2 Characteristics of ultrafast laser materials processing

Ultrafast laser materials processing has several distinct advantages over the conventional laser microfabrication techniques that generally employ continuous wave (CW) lasers or lasers with pulses longer than nanoseconds. First, ultrashort pulses significantly reduce the thermal effects in ultrafast laser processing, particularly when the peak intensity of the laser is controlled to be near the ablation threshold, and a sufficiently low repetition rate is used (e.g., a few kilohertz or a few tens of kilohertz). This is because when the laser pulse width is shorter than the electron-phonon coupling time of the laser-matter interactions, most of the laser energy is absorbed by the electrons and is very rapidly transferred to the lattice so that the energy is not dissipated through thermal diffusion [5, 8]. Therefore, the thermal diffusion to adjacent areas to the laser-irradiated region can effectively be ignored. This suppression of the HAZ enables the ultrafast lasers to be used to fabricate fine structures with microscale or nanoscale features.

Second, the ultrafast lasers can induce a strong absorption even in materials that are transparent to the laser frequency because of its unique nonlinear electron excitation mechanism [3, 4]. Figure 1 compares the single and multiphoton absorption processes that induce electron excitation. Conventional absorption involves linear single-photon absorption, which requires the photon energies that exceed the band gap of the material so that an electron can be excited from the valence band to the conduction band by absorbing a single photon (Figure 1A). Thus, light with the photon energies smaller than the band gap cannot directly excite the electrons. However, when an extremely high density of photons (i.e., extremely high intensity light) is incident on a material, an electron can be excited by the simultaneous absorption of multiple photons (Figure 1B). In such a case, the interaction between the ultrafast laser pulse and a transparent material can occur only near the focal point where the peak intensity is sufficiently high to initiate multiphoton absorption, as shown in Figure 1D. This important property is foundational for the 3D direct writing inside the transparent materials using the femtosecond laser pulses because there is virtually no out-of-focus absorption when a femtosecond laser beam is focused into a transparent bulk material. In contrast, for the long-pulsed or CW, the lasers can interact with the materials only by single-photon excitation making it impossible to internally modify the transparent materials due to surface absorption, as shown in Figure 1C.

Third, the combination of HAZ suppression and nonlinear multiphoton absorption in ultrafast laser processing enables a resolution far beyond the diffraction limit [6, 9]. As illustrated by the solid line in Figure 2, the intensity of an ultrafast laser beam will ideally have a Gaussian spatial profile. For a single-photon absorption, the spatial distribution of the laser energy absorbed by the material corresponds to this beam profile (FWHM beam diameter: ω_0).

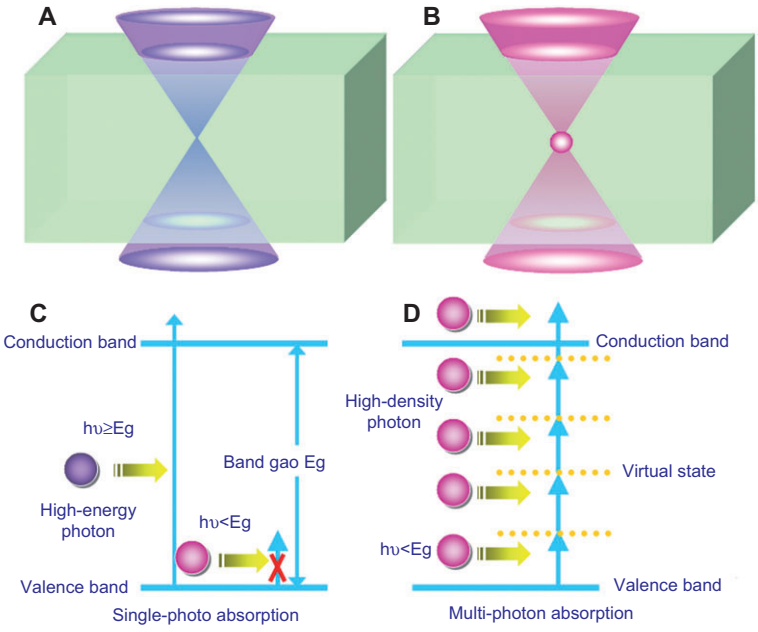

Figure 1 Laser processing of a transparent material by (A) single and (B) multiphoton absorption; their corresponding electron excitation processes are illustrated in (C) and (D), respectively.

However, the absorbed energy distribution will be narrower for multiphoton absorption as the effective absorption coefficient for *n*-photon absorption is proportional to the *n*th power of the laser intensity, as evidenced by the solid curve in Figure 2, which corresponds to the spatial distribution of the laser energy absorbed by a transparent material for the two-photon absorption. In addition, the fabrication resolution can be further improved by adjusting the laser intensity when there is a threshold laser intensity above which a reaction occurs on absorption. For example, when the laser energy is adjusted to match the threshold intensity for the reaction (indicated by the straight solid line in Figure 2), the fabrication resolution can be reduced to ~$0.54\times\omega_0$ as indicated in Figure 2. Thus, a resolution far beyond the diffraction limit can be achieved.

Finally, the ultrafast (particularly femtosecond) laser pulses can be used to finely tune or even completely alter the physical and chemical properties of a material in a spatially selective manner. Mainly due to this unique characteristic, the 3D femtosecond laser direct writing can integrate multiple functions on a single substrate [10–12].

3 Femtosecond laser processing systems

The femtosecond laser processing systems can be classified into two main categories: the femtosecond laser direct writing systems and the parallel femtosecond laser microprocessing systems. The femtosecond laser direct writing provides excellent fabrication flexibility, resolution, and quality and is particularly suitable for fabricating 3D microstructures within transparent materials. However, it suffers from a relatively low throughput as it is a serial fabrication process. Nevertheless, this problem has been significantly reduced due to rapid advances in high-average-power, high-repetition-rate femtosecond lasers in recent years. In contrast, the parallel femtosecond laser microprocessing approaches can realize high throughputs, but they frequently suffer from the reduced spatial resolution and sometimes lack the ability to fabricate structures with arbitrary 3D geometries (e.g., very often, parallel femtosecond laser processing techniques based on multiple beam interference or microlens arrays can fabricate only periodic structures). The selection of which approach to use depends on the requirements of the specific application.

3.1 Femtosecond laser direct writing systems

Figure 3 schematically shows a typical femtosecond laser direct writing system. The main components of this system are a femtosecond laser source, a beam control/shaping system, a microscope objective, or an aspherical lens for producing a tightly focused spot and a high-precision *XYZ* translation stage controlled by a computer for the 3D translation of the sample. The beam control/shaping system typically consists of an electro-optic or acoustic-optic device for controlling the repetition rate (e.g., a pulse picker) or creating a burst mode, a spatial or temporal pulse shaper, a tunable attenuator, and a mechanical shutter. In addition, a charge coupled device camera connected to a computer can be installed above the focusing lens to enable the fabrication process to be monitored in real time.

A key optical component in this system is the focusing lens because it determines the focal spot size, which is directly related to the fabrication resolution. As the femtosecond laser pulses possess a broad spectra, both spherical

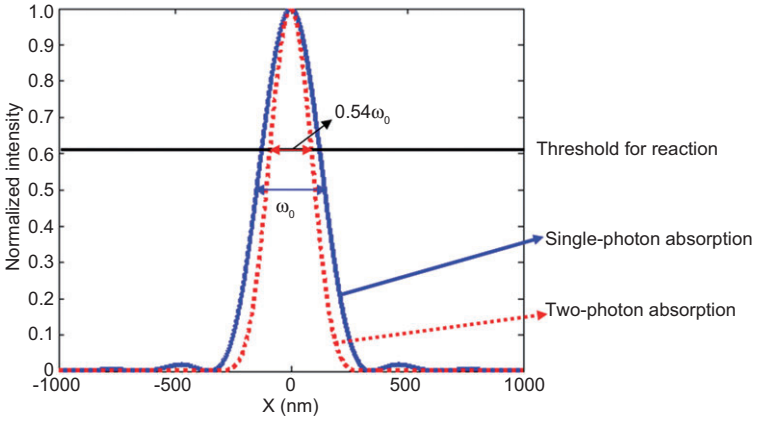

Figure 2 Actual beam profile (solid line) and spatial distributions of laser energy absorbed by transparent materials by two-photon (dashed line) absorption. The solid horizontal line indicates the reaction threshold.

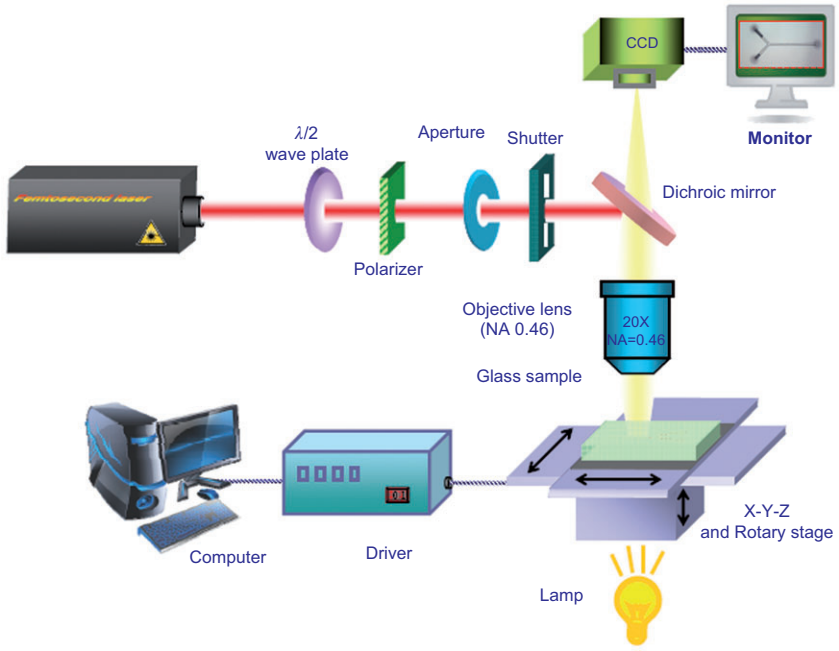

Figure 3 Schematic of the setup used for femtosecond laser direct writing.

and chromatic aberrations should be minimized when focusing them. For this reason, commercially available microscope objective lenses are frequently used for femtosecond laser processing, especially when high spatial resolutions are required. The fabrication resolution achievable with these objectives largely depends on their numerical aperture (NA), as in the lateral direction, the focal spot diameter is given by $1.22\lambda/\mathrm{NA}$, which is inversely proportional to the NA. However, a high-NA objective lens usually has a short working distance, limiting its ability to fabricate 3D microstructures deep in a substrate. Consequently, a trade off exists between the fabrication resolution and the working distance for each specific application. As a reference, in our previous studies, we often employed a relatively long working distance objective with an NA of 0.46 and a working distance of ~2 mm for writing optical waveguides and fabricating microfluidic channels in 2-mm-thick glass substrates [13]. On the other hand, very high NA objectives (e.g., oil immersion objectives) are often employed for surface nanostructuring or two-photon polymerization using femtosecond pulses because these applications do not require long working distances as they involve surfaces and thin samples [14, 15].

Another important optical component in the femtosecond laser direct writing systems is a tunable attenuator for externally controlling the femtosecond laser power. To ensure a stable operation (e.g., minimizing the fluctuations in the laser parameters such as the pulse width, pulse energy, and pointing direction), the output energy of the femtosecond laser will remain constant during fabrication. The pulse energy is usually varied by rotating a half-wave plate placed in front of a polarizer. If this combination of a half-wave plate and a polarizer does not allow the femtosecond laser pulses to be sufficiently attenuated because of the limited extinction ratio, neutral density filters can be inserted after the polarizer to achieve a wider tunable range.

In addition to the basic optical components mentioned above, a device for characterizing the spatiotemporal profiles of the femtosecond laser pulses is frequently required. To date, various devices have been developed for the characterization of the ultrafast laser pulses. In the simplest case, such a device can be an autocorrelator by which the temporal duration or structure of ultrashort pulses can be quantitatively evaluated with a moderate accuracy. The autocorrelator measures the femtosecond pulse duration by splitting the pulse into two replicas, mixing them in a nonlinear optical crystal, and recording the generated nonlinear signals (e.g., second or third harmonics) as a function of the relative delay between the two replicas. As the intensity of the nonlinear signal relies on the overlap between the two replicas, the temporal duration can be estimated from the autocorrelation trace by assuming a certain functional form for the temporal shape of the pulses to be measured. The autocorrelation measurement cannot provide information on the electric field. Extracting the complete information of the electric field is critical for understanding the mechanisms behind the interaction of the femtosecond

laser pulses with the materials, which can be achieved either by performing a spectrally resolved autocorrelation, which is termed frequency-resolved optical gating (FROG) or by measuring the spectral interference between two replicas of the test pulse whose frequencies are upconverted unevenly, which is termed spectral phase interferometry for direct electric-field reconstruction (SPIDER). For an overview of these common pulse characterization techniques, the readers can refer to some review articles, e.g., [16, 17]. Fortunately, the pulse characterization devices based on the above-mentioned techniques have all been commercialized today, which can be purchased depending on the requirements of the specific applications.

Most current pulse characterization techniques including the autocorrelation, FROG, and SPIDER can only be used to measure the temporal characteristics of the femtosecond pulses with a uniform temporal profile over the cross section of the laser beam. However, for investigating the microscopic processes involved in the femtosecond laser direct writing in various transparent materials, the direct characterization of the spatiotemporal profiles of the electric field of the tightly focused femtosecond laser pulses is sometimes more desirable, as in the focal volume, the spatiotemporal distortion of the pulses can easily occur due to the imperfection in the optical path alignment and/or the aberrations of the focusing systems. Such distortion can alter the laser-matter interaction at the microscopic scales, as discovered by Kazansky et al. [18]. In ambient air, the characterization of the femtosecond laser pulses at the focus can be realized by replacing the bulk nonlinear crystals used in the traditional techniques such as the FROG and SPIDER with nonlinear nanoprobes [19, 20]. However, the techniques enabling the characterization of the femtosecond laser pulses focused into the transparent materials are yet to be developed.

One drawback of the femtosecond laser direct writing is that it has a low throughput as it is a serial process. Fortunately, the compact, high-power, high-repetition rate ultrafast laser systems have recently been demonstrated, although their pulses are much broader than the pulses generated by the Ti:sapphire systems [21, 22]. With these lasers, the scan speed in direct writing can be dramatically increased by replacing the *XYZ* motion stage with a galvo scanner [23].

3.2 Parallel femtosecond laser microprocessing systems

Figure 4A–C schematically shows the three typical systems for parallel femtosecond microprocessing. Among them, the technique based on a microlens array shown in Figure 4A is a straightforward extension of the concept of the direct writing system described in Section 3.1 by spatially splitting the single focal spot into multiple foci uniformly distributed in the focal plane [24, 25]. The microlens array converts the collimated femtosecond laser beam into an array of focal spots in plane A. However, the focal spots in plane A will be too large due to the inherently low NA of the microlens. Therefore, a relay lens L1 followed by a high NA objective lens are used to project the focal spots formed in plane A onto the focal plane of the objective lens. This combination of a relay lens and an objective lens allows a fabrication resolution comparable to that of the objective lens to be realized. Figure 4D shows an array of the 3D microstructures (i.e., free-standing microsprings) fabricated by two-photon polymerization using a system similar to that in Figure 4A. In this case, over 200 focal spots are produced by a microlens array, which increased the yield efficiency by two orders of magnitude. To obtain a uniform intensity distribution in the focal spot array, the incident femtosecond laser was expanded before entering the microlens array. Amazingly, a subdiffraction-limited resolution of ~250 nm has been achieved with this system [25]. Previously, a major drawback of the multifocus parallel laser fabrication was that it could be used only for fabricating the microstructures arranged in periodic arrays. Obata et al. have recently developed a multifocus two-photon polymerization technique based on the individually controlled phase modulation that permits the rapid prototyping of the complex 2D and 3D structures (both symmetric and asymmetric structures) [26].

Parallel processing has also been demonstrated using multiple beam interference. This technique is potentially even faster than the microlens array-based laser direct writing because this technique can, in principle, be used to fabricate the periodic 2D/3D structures using only a single laser shot. These two techniques differ in that the microlens array-based laser direct writing can be used to fabricate the structures with arbitrary 3D geometries in each unit cell, whereas the multiple-beam interference technique cannot. A typical parallel laser processing system based on multiple-beam interference is shown in Figure 4B, in which a diffraction optical element (DOE) first splits the incident beam into five perfectly synchronized beamlets [27]. These diverging beamlets are then collimated by a lens. Before these beamlets are refocused into the sample by a second lens to create the interference patterns, the phase and amplitude of each of beamlet can be tuned using phase retarders (as shown in Figure 4B) and attenuators. This has enabled a rich variety of interference patterns to be generated in 2D and 3D spaces

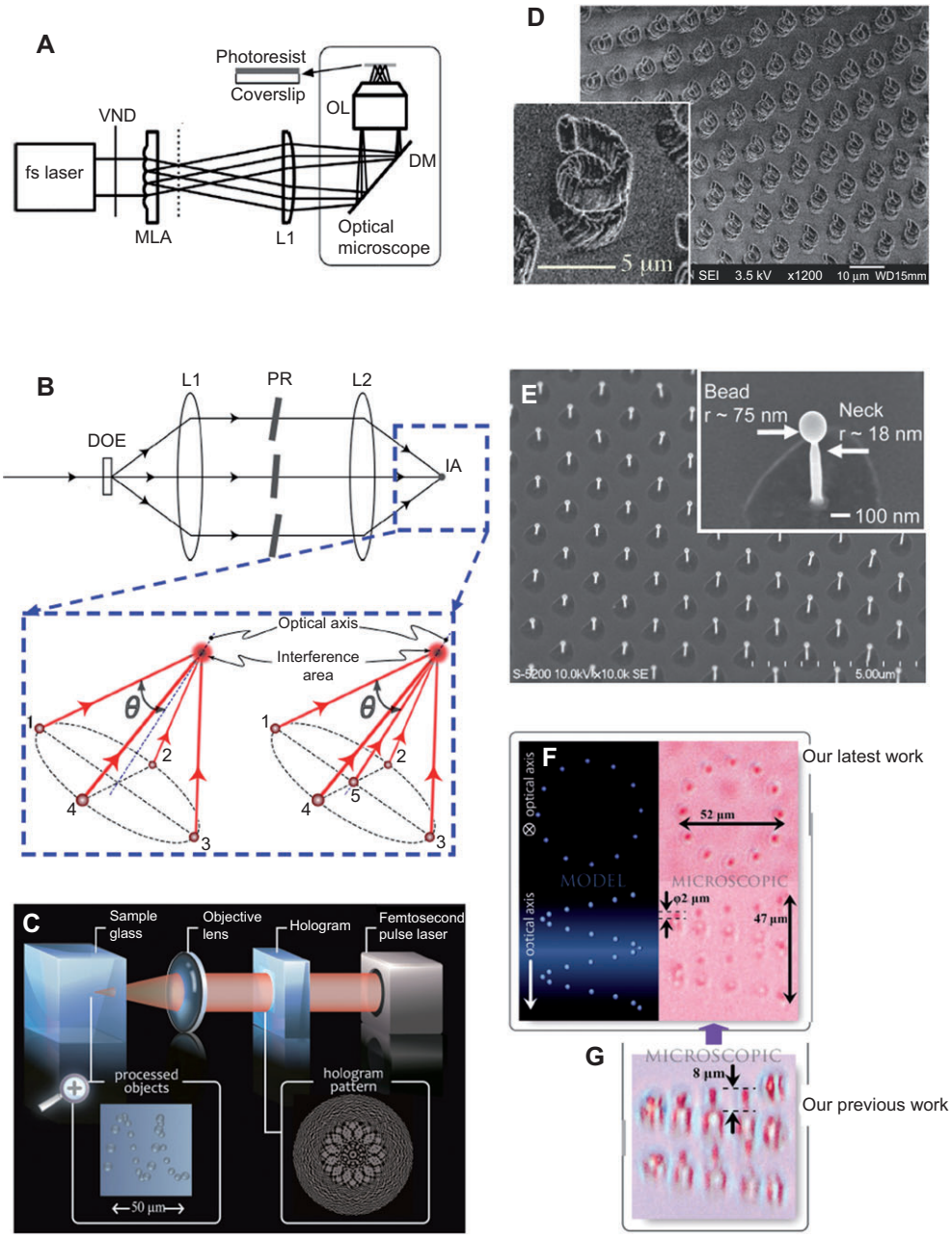

Figure 4 (A) Optical setup for multifocus parallel laser writing [24] (courtesy of S. Matsuo). (B) Optical setup for parallel laser processing based on multiple-beam interference [27] (courtesy of H. Misawa). (C) Optical setup for parallel laser processing using a hologram [31] (courtesy of M. Yamaji, K. Miura, and K. Hirao). (D) 3D microsprings arranged in an array fabricated using a system similar to that in (A) [25] (courtesy of J. Kato). (E) An array of nanodroplets fabricated on gold thin film by interference between four femtosecond laser beams [29] (courtesy of Y. Nakata). (F) 3D microstructures fabricated using the system in (C) [31] (courtesy of M. Yamaji, K. Miura, and K. Hirao).

[28, 29]. Figure 4E shows that an array of nanodroplets formed on the gold thin films processed by the interference of four femtosecond laser beams with a pulse length of ~130 fs at a central wavelength of ~790 nm (i.e., the zeroth-order diffraction beam of the DOE is blocked). As the inset in Figure 4E shows, the stem under the nanobead has a diameter of only ~36 nm, and the diameter of the nanobead is ~150 nm [29].

To fabricate the non-periodic microstructures by parallel femtosecond laser processing, the system in Figure 4B can be modified by replacing the DOE with a hologram [e.g., either etched in a transparent glass substrate or formed on a reflective spatial light modulator (SLM)], as illustrated in Figure 4C [30, 31]. However, this technique often suffers from a poor axial resolution due to the small convergence angle of the refocused diffraction

beams from the hologram. This situation has recently been much improved by Yamaji et al. [31]. They achieved the homogeneous and elongation-free 3D microfabrication with this technique by carefully controlling the peak intensity of the laser pulses and the focal length of the hologram, as shown in Figure 4F. For comparison, an earlier result of fabricating the same structure is presented in Figure 4G; the former exhibits a far inferior axial resolution.

4 Optics for laser pulse shaping

Owing to its non-thermal, heat diffusion-free characteristics, the subdiffraction-limited spatial resolution of the femtosecond laser processing is highly sensitive to the spatial profile of the focal spot. The spatial shaping of the femtosecond laser pulses has been used to demonstrate the focal spot engineering with a spatial resolution on the wavelength scales. On the other hand, the short pulse widths, which result in broad spectra, facilitate temporal shaping of the femtosecond laser pulses on the time scale of transient electron dynamics. This section discusses the basic concepts of pulse shaping and the typical optical devices and systems used to realize it.

4.1 Optics for temporal pulse shaping

The temporal shaping of the femtosecond laser pulses is usually performed in the frequency domain, as schematically illustrated in Figure 5A. A typical optical system for temporal pulse shaping consists of a pair of gratings and a pair of focusing lenses, which are arranged in a 4-f configuration for zero dispersion. A pulse-shaping mask, which can be an SLM, a deformable mirror, or an acoustic-optical modulator, is placed in the Fourier plane for tuning the spectral phase and/or amplitude [32, 33]. This simple, yet powerful, device can generate almost arbitrary pulse profiles with a resolution (e.g., finest temporal feature) that is limited only by the spectral width of the pulses, enabling photoionization and electron-electron impact ionization to be controlled even on intrinsic time and intensity scales [34]. For experiments involving complex nonlinear interactions, it is frequently difficult to predict the optimal temporal profiles by theory. In such cases, a self-learning, adaptive loop can be incorporated in the pulse shaper to optimize the temporal profile of the pulse based on the targets of specific applications. Figure 5B shows that deep channels can be drilled into fused silica with a few cracks

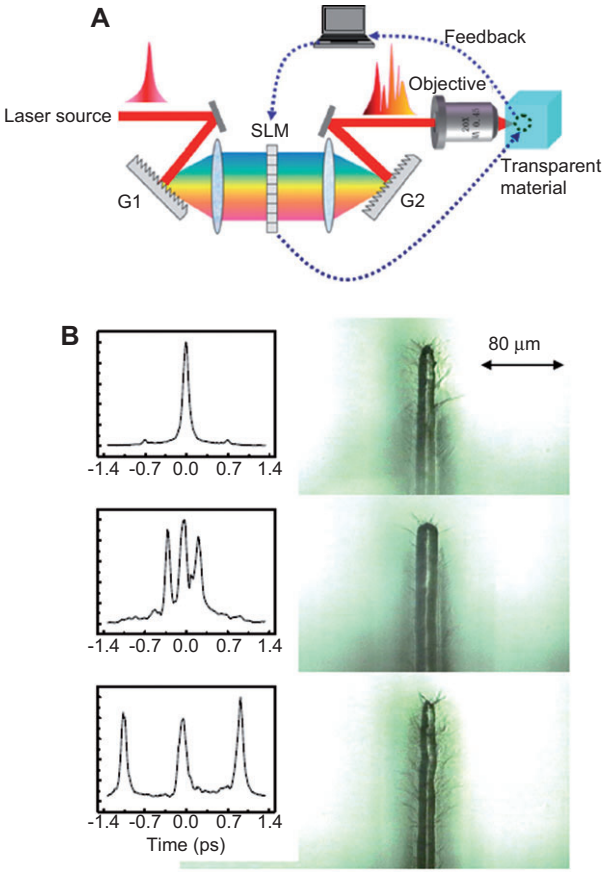

Figure 5 (A) Schematic illustration of a temporal pulse-shaping system with an adaptive self-learning loop. (B) Microchannels drilled in glass substrates using a transform-limited pulse (upper panel), a train of three pulses separated by ~300 fs (middle panel), and a train of three pulses separated by ~1 ps (lower panel) [7] (courtesy of R. Stoian).

and a low surface roughness by replacing a transform-limited femtosecond laser pulse with shaped pulses of a temporal profile consisting of a train of three intensity spikes with similar amplitudes and a separation of ~300 fs, whereas further increasing the separation to ~1 ps again leads to poor fabrication quality [7]. In addition, temporally shaped asymmetrical pulse trains have been used to realize the nanoscale (~100 nm in diameter) ablation of fused silica [34].

4.2 Optics for spatial pulse shaping

In its most general sense, spatial pulse shaping includes any modification of the phase or amplitude of the incident laser beam before it enters the focusing lens. Thus, the techniques described in Section 3.2 all belong to this category. Other examples include the use of Bessel

beams of the femtosecond laser for drilling deep channels in glass [35, 36]. In this section, we mainly focus on the spatial pulse-shaping techniques that are used to improve the optical resolutions of the laser direct writing systems (e.g., engineering the focal spot). This is because, unlike conventional planar lithography in which the feature size is solely determined by the lateral resolution, the spatial resolutions in all the three dimensions have to be taken into account in the femtosecond laser 3D direct writing. Unfortunately, the focal spots produced by the objective lenses naturally have asymmetrical shapes that are elongated in the propagation direction, resulting in widely differing lateral and axial resolutions.

Several beam-shaping techniques have been developed to solve this problem [37–41]. For instance, in the widely used transverse writing scheme (i.e., the writing direction is perpendicular to the direction of the laser propagation), balanced lateral and axial resolutions can be realized by shaping the input femtosecond laser beams using a pair of cylindrical lenses [37] or a narrow slit [38–40] placed before the objective lens or by combining two temporally overlapped, crossed femtosecond laser beams [41]. Among these techniques, the slit-beam shaping method has received considerable attention for fabricating microfluidic channels and writing waveguides because of its simplicity and effectiveness. Figure 6A schematically illustrates the focusing system that contains a narrow slit that can be placed over the objective lens without using an extra mount. It is important that the slit is oriented parallel to the direction of the sample motion in the laser writing process. Figure 6B shows that a single-mode waveguide fabricated using slit-beam shaping has a perfectly circular cross section with a diameter of <15 μm, whereas the cross section of the waveguide produced by normal focusing without using the slit is highly asymmetric and significantly elongated in the laser propagation direction [39].

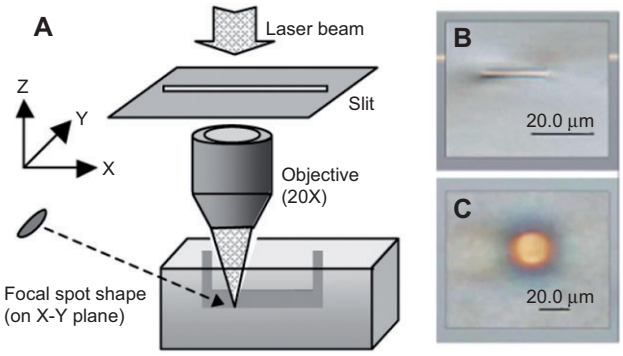

Figure 6 (A) Schematic illustration of the slit-beam shaping system [38]. (B) Optical waveguides written in glass without (upper panel) and with (lower panel) slit-beam shaping [39] (reproduced with permission from OSA ©2005 by the Optical Society of America).

4.3 Optics for spatiotemporal pulse shaping

Spatiotemporal pulse-shaping techniques, which were originally developed by scientists in the field of bioimaging [42, 43], have recently attracted significant attention for improving the performance of 3D femtosecond laser processing [44–52]. Figure 7A shows a typical spatiotemporal pulse-shaping system in which the incident pulses are first spatially dispersed by a pair of parallel gratings before entering the focusing lens. Temporal focusing occurs because the spatial overlapping of the different frequency components only occurs around the focus, resulting in the shortest pulse width and, hence, the highest peak intensity. This will improve the axial resolution of the femtosecond laser microfabrication because the peak intensity will decrease rapidly due to the broadening of the pulse width when moving away from the geometric focal spot [44–46]. This also suppresses the nonlinear propagation effects (e.g., filamentation and self-focusing), which can hinder the fabrication of the 3D structures in the thick samples with low-NA focusing lenses. This can be clearly seen in Figure 7B, which shows that a filament is formed throughout a 6-mm-thick fused silica. In such a case, space-selective

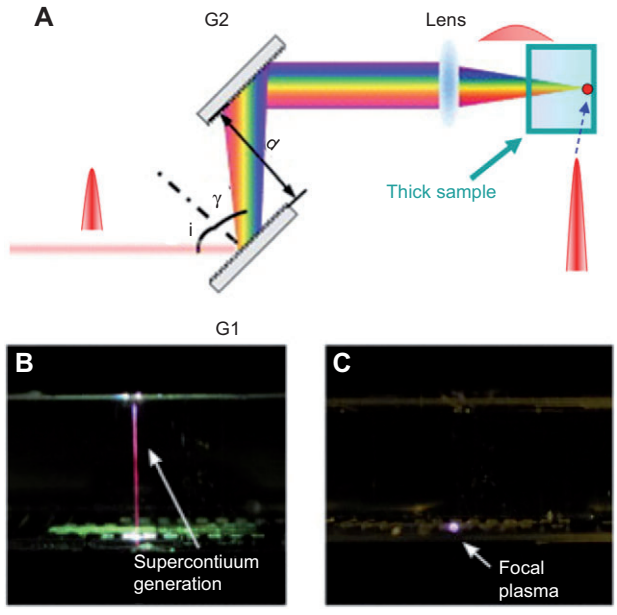

Figure 7 (A) Schematic illustration of a typical spatiotemporal pulse-shaping system [45]. Focusing femtosecond laser pulses into thick glass samples (B) with and (C) without spatiotemporal pulse shaping using a low-NA focusing lens [47] (reproduced with permission from OSA ©2010 by the Optical Society of America).

fabrication in the axial direction is impossible. Amazingly, with spatiotemporal shaping, a tightly confined 3D focal spot can be realized at the bottom of a glass substrate, as shown in Figure 7C [47]. This unique characteristic makes spatiotemporal shaping very attractive for fabricating large-scale 3D structures inside thick substrates.

An exotic aspect of the spatiotemporal focusing is that it can naturally form a tilted pulse front, as first pointed out by Vitek et al. [48]. Remarkably, the tilting angle can be precisely controlled in a wide range by adjusting the spatial chirp of the incident beam at the entrance of the objective lens [45, 46, 48]. It has been found that the pulse-front tilt can induce the so-called 'quill writing' effect in femtosecond laser processing, i.e., the laser-induced modifications in homogeneous materials show a remarkable change when the writing direction is reversed [18]. The microscopic mechanism underlying this effect has not yet been fully understood, whereas it seems to be closely linked to the structure existing in the electron plasma [18, 49, 50]. The 'quill writing' effect opens new opportunities for controlling nano-texture formation in processed materials, which has important consequences on various applications such as the writing of waveguides and polarization-sensitive devices, and the fabrication of microfluidic channels.

4.4 Optics for pulse polarization control

As a final example of pulse shaping, we discuss the optics for controlling pulse polarization. The importance of the polarization of the writing laser beam on the modified structure was noticed in 1999 when Kazansky et al. discovered an anisotropic light scattering in Ge-doped silica glass irradiated by a femtosecond laser beam [53], and Sudrie et al. observed a permanent birefringence induced by the femtosecond laser in fused silica [54]. It was subsequently clarified that nanograting-like structures oriented perpendicularly to the polarization of the writing laser are induced in transparent materials and that they are responsible for the observed macroscopic birefringence phenomena [55, 56]. This formation of subwavelength-scale nanograting structures has been exploited in the fabrication of microfluidic structures [57] and polarization-sensitive optical components [58–60].

Figure 8A illustrates a sophisticated polarization control system in which the time delay between two cross-polarized pulses can be continuously controlled with high precision [60]. This has enabled a continuous rotation of the azimuth angle of the birefringence (i.e., the slow axis) of the laser-inscribed structure, as shown in Figure 8B. Figure 8C shows a tiny world map printed in fused silica

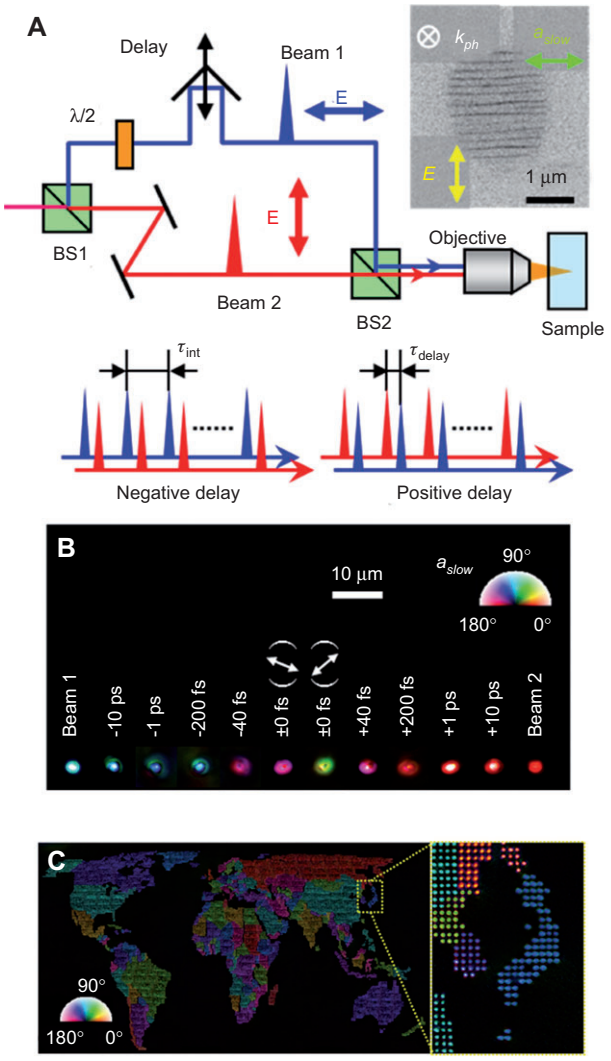

Figure 8 (A) Schematic illustration of cross-polarized double-pulse femtosecond laser writing setup (upper panel), and the pulse diagrams of the double pulse experiments (lower panel). (B) Typical microscopy images of localized birefringence taken with polarization optical microscope (pseudo-color indicates the direction of the slow axis, see polar legend). (C) Image of a tiny 'world map' written in glass using the system in (A), taken with polarization (azimuth angle) microscopes [60] (courtesy of Y. Shimotsuma, K. Miura, and K. Hirao).

using delay-tunable cross-polarized double pulses. Under a polarization microscope, this map exhibits different colors renderings due to the pseudo-color mapping of the azimuth angle of the slow axis [60].

5 Summary and outlook

We have given an overview of the basic concepts, the characteristics, and the typical systems for ultrafast laser

materials processing. In particular, the typical optical devices and systems for spatial and temporal shaping of the femtosecond laser pulses and pulse polarization control have been reviewed. The use of the state-of-the-art pulse shaping optics has enabled the focal spot to be tailored in 3D space on a wavelength scale and ultrafast control of the dynamics of energy deposition into materials on time scales shorter than the electron-phonon coupling time. These unique properties make the ultrafast lasers indispensable processing tools for a wide variety of applications, especially when precision and surface quality are critical.

Since its birth, the field of ultrafast laser materials processing has benefited from the rapid development of the ultrafast laser systems and the ultrafast laser techniques. For example, the temporal pulse-shaping technique described in Section 4.1 was originally developed for the coherent control of the dynamics of the quantum systems (e.g., the outcome of a photochemical reaction) on ultrafast time scales [61]. A future opportunity to further exploit the cutting-edge ultrafast laser technology is to employ the few-cycle pulses in materials processing, as has been demonstrated by a few groups [62, 63]. As the few-cycle pulses have very broad spectra, special care is required to compensate their dispersion. In addition, the interaction of the few-cycle pulses with matter is often sensitive to the carrier envelop phase (i.e., the relative phase between the peak of the pulse envelope and the underlying electric field carrier wave), which adds a new dimension to the parameter space. Currently, dispersion control optics include gratings and chirped mirrors, whereas the control of the carrier envelop phase of the few-cycle pulses is usually achieved by tuning the separation between a pair of glass wedges inserted in the optical path [64].

For resolution enhancement, ultrafast laser materials processing has benefited from the research in 3D bioimaging. For example, stimulated emission depletion (STED), has enabled a sub-10-nm resolution to be achieved in far-field imaging [65], and it has been employed in the femtosecond laser 3D nanofabrication by two-photon polymerization [66, 67]. In addition, the spatiotemporal focusing techniques, which were originally developed for reducing out-of-focus noise [42] and enhancing the imaging speed [43] of multiphoton microscopy, have been employed in shaping the focal spot [44–46] and increasing the 3D fabrication throughput [51, 52]. On the other hand, the concepts originally considered for achieving the subdiffraction-limited resolutions in the ultrafast laser processing have inspired the development of new techniques for super-resolution bioimaging. For example, a fluorescent label exhibiting a nonlinear thresholding effect (see Section 2 and Figure 2) in its response to linear light excitation has recently been designed to realize super-resolution far-field imaging using a conventional confocal microscope [68]. The exchange of ideas and the interaction between these two closely related fields should be further promoted in the future.

In the more distant future, ultrafast laser materials processing may use attosecond (10^{-18} s) laser pulses, as suggested by Corkum's group [69]. The attosecond laser pulses are capable of controlling the electron dynamics on time scales of electron motion in or between atoms. In addition, the attosecond pulses often lie in the extreme ultraviolet (EUV) or even the soft X-ray region and thus have shorter wavelengths than the femtosecond laser pulses in the visible or near-infrared region. Consequently, they have the potential to be focused to smaller spots according to Abbe's law. To this end, the optical components in the EUV region need to be developed to steer, focus, and realize the spectral and dispersion control of the attosecond pulses.

Received July 9, 2012; accepted August 19, 2012

References

[1] R. Srinivasan, E. Sutcliffe and B. Braren, Appl. Phys. Lett. 51, 1285–1287 (1987).
[2] S. Küper and M. Stuke, Appl. Phys. B 44, 199–204 (1987).
[3] K. M. Davis, K. Miura, N. Sugimoto and K. Hirao, Opt. Lett. 21, 1729–1731 (1996).
[4] E. N. Glezer, M. Milosavljevic, L. Huang, R. J. Finlay, T. H. Her, et al., Opt. Lett. 21, 2023–2025 (1996).
[5] C. Momma, B. N. Chichkov, S. Nolte, F. Alvensleben, A. Tünnermann, et al., Opt. Commun. 129, 134–142 (1996).
[6] A. P. Joglekar, H. Liu, E. Meyhöfer, G. Mourou and A. J. Hunt, Proc. Natl. Acad. Sci. USA 101, 5856–5861 (2004).
[7] R. Stoian, M. Boyle, A. Thoss, A. Rosenfeld, G. Korn, et al., Appl. Phys. Lett. 80, 353–355 (2002).
[8] S. I. Anisimov and B. Rethfeld, Proc. SPIE 3093, 192–203 (1997).
[9] S. Kawata, H. B. Sun, T. Tanaka and K. Takada, Nature 412, 697–698 (2001).
[10] K. Sugioka and Y. Cheng, MRS Bull. 36, 1020–1027 (2011).
[11] R. Osellame, H. J. W. M. Hoekstra, G. Cerullo and M. Pollnau, Laser Photonics Rev. 5, 442–463 (2011).
[12] K. Itoh, W. Watanabe, S. Nolte and C. Schaffer, MRS Bull. 31, 620–625 (2006).

[13] K. Sugioka, Y. Cheng and K. Midorikawa, Appl. Phys. A 81, 1–10 (2005).
[14] M. Straub, M. Afshar, D. Feili, H. Seidel and K. König, Opt. Lett. 37, 190–192 (2012).
[15] L. Li and J. T. Fourkas, Mater. Today 10, 30–37 (2007).
[16] I. A. Walmsley and C. Dorrer, Adv. Opt. Photon. 1, 308–437 (2009).
[17] A. Monmayrant, S. Weber and B. Chatel, J. Phys. B: At. Mol. Opt. Phys. 43, 103001 (2010).
[18] P. G. Kazansky, W. Yang, E. Bricchi, J. Bovatsek, A. Arai, et al., Appl. Phys. Lett. 90, 151120 (2007).
[19] P. Bowlan, U. Fuchs, R. Trebino and U. D. Zeitner, Opt. Express 16, 13663 (2008).
[20] H. F. Li, Z. Zhang, Q. Xu, K. B. Shi, Y. S. Jia, et al., Appl. Phys. Lett. 97, 261108 (2010).
[21] S. V. Marchese, C. R. E. Baer, A. G. Engqvist, S. Hashimoto, D. J. H. C. Maas, et al., Opt. Express 16, 6397–6407 (2008).
[22] J. Kleinbauer, D. Eckert, S. Weiler and D. H. Sutter, Proc. SPIE 6871, 68711B (2008).
[23] M. Mielke, D. Gaudiosi, K. Kim, M. Greenberg, X. Gu, et al., J. Laser Micro/Nanoeng. 5, 53–58 (2010).
[24] S. Matsuo, T. Miyamoto, T. Tomita and S. Hashimoto, Appl. Opt. 46, 8264–8267 (2007).
[25] J. Kato, N. Takeyasu, Y. Adachi, H. Sun and S. Kawata, Appl. Phys. Lett. 86, 044102 (2005).
[26] K. Obata, J. Koch, U. Hinze and B. N. Chichkov, Opt. Express 18, 17193–17200 (2010).
[27] T. Kondo, S. Juodkazis, V. Mizeikis, S. Matsuo and H. Misawa, New J. Phys. 8, 250 (2006).
[28] K. K. Seet, V. Jarutis, S. Juodkazis and H. Misawa, Proc. SPIE 6050, 60500S (2005).
[29] Y. Nakata, N. Miyanaga and T. Okada, Appl. Surf. Sci. 253, 6555–6557 (2007).
[30] S. Hasegawa, Y. Hayasaki and N. Nishida, Opt. Lett. 31, 1705–1707 (2006).
[31] M. Yamaji, H. Kawashima, J. Suzuki, S. Tanaka, M. Shimizu, et al., J. Appl. Phys. 111, 083107 (2012).
[32] A. M. Weiner, Rev. Sci. Instrum. 71, 1929–1960 (2000).
[33] R. Stoian, Top. Appl. Phys. 123, 67–91 (2012).
[34] L. Englert, B. Rethfeld, L. Haag, M. Wollenhaupt, C. Sarpe-Tudoran, et al., Opt. Express 15, 17855–17862 (2007).
[35] M. K. Bhuyan, F. Courvoisier, P. A. Lacourt, M. Jacquot, L. Furfaro, et al., Opt. Express 18, 566–574 (2010).
[36] M. K. Bhuyan, F. Courvoisier, P. A. Lacourt, M. Jacquot, R. Salut, et al., Appl. Phys. Lett. 97, 081102 (2010).
[37] G. Cerullo, R. Osellame, S. Taccheo, M. Marangoni, D. Polli, et al., Opt. Lett. 27, 1938–1940 (2002).
[38] Y. Cheng, K. Sugioka, K. Midorikawa, M. Masuda, K. Toyoda, et al., Opt. Lett. 28, 55–57 (2003).
[39] M. Ams, G. Marshall, D. Spence and M. Withford, Opt. Express 13, 5676–5681 (2005).
[40] S. Sowa, W. Watanabe, T. Tamaki, J. Nishii and K. Itoh, Opt. Express 14, 291–297 (2006).
[41] K. Sugioka, Y. Cheng, K. Midorikawa, F. Takase and H. Takai, Opt. Lett. 31, 208–210 (2006).
[42] G. Zhu, J. van Howe, M. Durst, W. Zipfel and C. Xu, Opt. Express 13, 2153–2159 (2005).
[43] D. Oron, E. Tal and Y. Silberberg, Opt. Express 13, 1468–1476 (2005).
[44] F. He, H. Xu, Y. Cheng, J. Ni, H. Xiong, et al., Opt. Lett. 35, 1106–1108 (2010).
[45] F. He, Y. Cheng, J. T. Lin, J. L. Ni, Z. Z. Xu, et al., New J. Phys. 13, 083014 (2011).
[46] C. G. Durfee, M. Greco, E. Block, D. Vitek and J. A. Squier, Opt. Express 20, 14244–14259 (2012).
[47] D. N. Vitek, D. E. Adams, A. Johnson, P. S. Tsai, S. Backus, et al., Opt. Express 18, 18086–18094 (2010).
[48] D. N. Vitek, E. Block, Y. Bellouard, D. E. Adams, S. Backus, et al., Opt. Express 18, 24673–24678 (2010).
[49] W. J. Yang, P. G. Kazansky and Y. P. Svirko, Nat. Photonics 2, 99–104 (2008).
[50] B. Poumellec, M. Lancry, J. C. Poulin and S. Ani-Joseph, Opt. Express 16, 18354–18361 (2008).
[51] D. Kim and P. T. C. So, Opt. Lett. 35, 1602–1604 (2010).
[52] Y. C. Li, L. C. Cheng, C. Y. Chang, C. H. Lien, P. J. Campagnola, et al., Opt. Express 20, 19030–19038 (2012).
[53] P. G. Kazansky, H. Inouye, T. Mitsuyu, K. Miura, J. Qiu, et al., Phys. Rev. Lett. 82, 2199–2202 (1999).
[54] L. Sudrie, M. Franco, B. Prade and A. Mysyrowicz, Opt. Commun. 171, 279–284 (1999).
[55] Y. Shimotsuma, P. G. Kazansky, J. Qiu and K. Hirao, Phys. Rev. Lett. 91, 247405 (2003).
[56] V. R. Bhardwaj, E. Simova, P. P. Rajeev, C. Hnatovsky, R. S. Taylor, et al., Phys. Rev. Lett. 96, 057404 (2006).
[57] C. Hnatovsky, R. Taylor, E. Simova, V. Bhardwaj, D. Rayner, et al., Opt. Lett. 30, 1867–1869 (2005).
[58] M. Beresna, M. Gecevičius and P. G. Kazansky, Opt. Mater. Express 1, 783–795 (2011).
[59] M. Huang, F. L. Zhao, Y. Cheng, N. S. Xu and Z. Z. Xu, Opt. Express 16, 19354–19365 (2008).
[60] Y. Shimotsuma, M. Sakakura, P. G. Kazansky, M. Beresna, J. Qiu, et al., Adv. Mater. 22, 4039–4043 (2010).
[61] C. Brif, R. Chakrabarti and H. Rabitz, New J. Phys. 12, 075008 (2010).
[62] N. Sanner, O. Utéza, B. Chimier, M. Sentis, P. Lassonde, et al., Appl. Phys. Lett. 96, 071111 (2010).
[63] L. Hoffart, P. Lassonde, F. Légaré, F. Vidal, N. Sanner, et al., Opt. Express 19, 230–240 (2011).
[64] T. Fuji, J. Rauschenberger, A. Apolonski, V. S. Yakovlev, G. Tempea, et al., Opt. Lett. 30, 332–334 (2005).
[65] E. Rittweger, K. Y. Han, S. E. Irvine, C. Eggeling and S. W. Hell, Nat. Photonics 3, 144–147 (2009).
[66] L. Li, R. R. Gattass, E. Gershgoren, H. Hwang and J. T. Fourkas, Science 324, 910–913 (2009).
[67] J. Fischer and M. Wegener, Opt. Mater. Express 1, 614–624 (2011).
[68] J. F. Chen and Y. Cheng, Opt. Lett. 34, 1831–1833 (2009).
[69] D. Grojo, M. Gertsvolf, S. Lei, T. Barillot, D. M. Rayner, et al., Phys. Rev. B 81, 212301 (2010).

Koji Sugioka received his BS, MS. Eng., and Dr. Eng. degrees from Waseda University in 1984, 1986, 1993, respectively. He is now a senior research scientist in RIKEN and a guest professor at Tokyo University of Science and Tokyo Denki University. His current research interests focus on ultrafast laser processing for microfluidic and optofluidic applications and optoelectronics applications. He is currently a member of the board of directors of Laser Institute of America (LIA) and Japanese Laser Processing Society (JLPS), and a SPIE Fellow.

Ya Cheng received his BS degree from the Fudan University in 1993, and his PhD degree from the Shanghai Institute of Optics and Fine Mechanics (SIOM), Chinese Academy of Sciences in 1998. He is now a professor of SIOM. His research activity has mainly focused on nonlinear optics and applications of ultrashort laser pulses. His current research interests include femtosecond laser micromachining of glass materials for microfluidic and optofluidic applications and ultrafast nonlinear optics in tunnel ionization regime. He is a Fellow of the Institute of Physics – London.